SATURATED PROPORTIONAL DERIVATIVE CONTROL OF A SINGLE-LINK FLEXIBLE-JOINT MANIPULATOR

Ryan James Caverly[1], David Evan Zlotink[1], James Richard Forbes[2]
[1]*Research Assistant, Department of Mechanical Engineering, McGill University, Montreal, QC, Canada*
[2]*Assistant Professor, Department of Mechanical Engineering, McGill University, Montreal, QC, Canada*
Email: ryan.caverly@mail.mcgill.ca; david.zlotnik@mail.mcgill.ca; james.richard.forbes@mcgill.ca

ABSTRACT

This paper considers the control of a single-link flexible-joint robotic manipulator subject to actuator saturation. Several alternative controllers are proposed and compared to one found in literature. In particular, a controller with proportional and derivative components is guaranteed to provide a total torque less than a chosen value thereby disallowing actuator saturation. It is shown that an equilibrium point of the closed-loop system is asymptotically stable. Additionally, it is shown that the controllers are robust to modelling errors. Finally, this paper presents experimental results demonstrating the proposed control architecture.

Keywords: proportional derivative control; saturation avoidance; flexible-joint manipulator.

LE CONTRÔLE PROPORTIONNEL DÉRIVÉ SATURÉ D'UN MANIPULATEUR À JOINT FLEXIBLE

RÉSUMÉ

Ce papier, considère le contrôle d'un manipulateur robotique à joint flexible sujet à la saturation d'actuateur. Plusieurs contrôleurs alternatifs sont proposés et comparés à un contrôleur dans la litérature. En particulier, un controleur avec une portion proportionnelle et une portion dérivée, qui garanti un moment de torsion total moins qu'une valeur spécifiée. Il est démontreé qu'un point d'équilibre du système à circuit fermé est asymptotiquement stable. En plus, il est attesté que les contrôleurs sont robustes aux erreurs de modélisation. Finalement, ce papier présente des résultats expérimentaux qui illustrent l'application des contrôleurs proposés.

Mots-clés : contrôle proportionnel dérivé ; l'évitement de saturation ; manipulateur à joint flexible.

1. INTRODUCTION

Robot manipulators are used in many branches of manufacturing for tasks such as robotic welding and automated assembly. The flexibility of manipulator joints is often left unmodelled and uncontrolled, leading to performance limitations [1, 2]. This flexibility is caused by the gears and belts used to transmit the torque produced by the actuators to the links [2]. Often the natural frequencies of these joints are relatively low ($2-3$ Hz), which coincide with the frequency of the trajectory being followed, forcing the operator to wait for any vibrations to decay naturally [3]. Moreover, in large robotic manipulators, such as the Canadarm, even a relatively small joint flexibility can cause significant vibrations at the manipulator tip, which is highly undesirable. Several authors have investigated the modelling and control of flexible-joint robotic manipulators using widely varying techniques [4–8].

Actuator limitations also become a factor when controlling flexible-joint robotic manipulators. Powerful motors are generally large and heavy which is undesirable; the increased mass of the system results in increased power requirements, as well as possible performance limitations [9]. For this reason, somewhat smaller or at least modestly sized motors are used in practice, resulting in limited joint torques. As such, avoiding actuator saturation while simultaneously assuring asymptotic stability of the closed-loop equilibrium point is of great interest. In the context of robotic manipulators, various authors have studied saturation avoidance [10–12]. Spacecraft attitude control accounting for actuator saturation has also been investigated in [13–15]. In particular, in [13] a simple proportional derivative (PD) type control law that explicitly accounts for actuator saturation is presented.

The novel contribution of this paper is adopting and building upon [13] by designing and analyzing PD control laws specifically for a single-link flexible-joint robotic manipulator. Specifically, four PD controllers will be considered that disallow actuator saturation and simultaneously guarantee asymptotic stability of the equilibrium point of the closed-loop system. Additionally, experimental validation of the proposed controllers will be performed, and they will be compared to an existing controller found in the literature.

The remainder of this paper is as follows. In Section 2 the dynamics of a one-link flexible robotic manipulator are derived. In Section 3 the proposed controllers are presented and shown to be asymptotically stable, even in the presence of parameter uncertainty. Section 4 presents experimental results, thus validating the proposed controllers, and some final remarks are given in Section 5.

2. SYSTEM DYNAMICS

Consider the single-link flexible-joint robotic manipulator shown in Fig. 1. The kinetic and potential energies, as well as the Rayleigh dissipation function, respectively are

$$T = \tfrac{1}{2}\dot{\mathbf{q}}^{\mathsf{T}}\mathbf{M}\dot{\mathbf{q}},$$

$$U = \tfrac{1}{2}\mathbf{q}^{\mathsf{T}}\mathbf{K}\mathbf{q},$$

$$R = \tfrac{1}{2}\dot{\mathbf{q}}^{\mathsf{T}}\mathbf{D}\dot{\mathbf{q}},$$

where $\mathbf{M} = \mathbf{M}^{\mathsf{T}} > 0$ is the system's mass matrix, $\mathbf{K} = \mathbf{K}^{\mathsf{T}} \geq 0$ is the system's stiffness matrix, $\mathbf{D} = \mathbf{D}^{\mathsf{T}} > 0$ is the system's damping matrix, and $\mathbf{q} = \begin{bmatrix}\theta & \alpha\end{bmatrix}^{\mathsf{T}}$ is the generalized coordinate of the system. The angle θ is the angle of the base hub relative to a fixed inertial frame and α is the angle of the manipulator link relative to the base hub. Using a Lagrangian approach, the equations of motion can be found to be

$$\mathbf{M}\ddot{\mathbf{q}} + \mathbf{D}\dot{\mathbf{q}} + \mathbf{K}\mathbf{q} = \hat{\mathbf{b}}\tau_c, \tag{1}$$

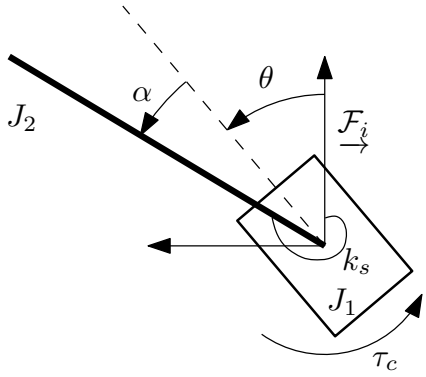

Fig. 1. Schematic of a flexible-joint.

where $\hat{\mathbf{b}}$ is the matrix that distributes the applied torque to the system and τ_c is the torque input to the system. The mass, stiffness, damping, and input matrices of our system are

$$\mathbf{M} = \begin{bmatrix} J_1 + J_2 & J_2 \\ J_2 & J_2 \end{bmatrix}, \quad \mathbf{K} = \begin{bmatrix} 0 & 0 \\ 0 & k_s \end{bmatrix}, \quad \mathbf{D} = \begin{bmatrix} d_1 & 0 \\ 0 & d_2 \end{bmatrix}, \quad \hat{\mathbf{b}} = \begin{bmatrix} 1 \\ 0 \end{bmatrix},$$

where J_1, J_2 are the moment of inertias of the manipulator hub and link respectively, k_s is the torsional spring constant between the hub and link, and d_1, d_2 are the damping coefficients of the hub and link respectively.

3. CONTROL FORMULATION

3.1. Control Law

Consider the following PD control law:

$$\tau_c = u_p + u_d,$$

where u_p is proportional control and u_d is derivative control. The authors of [11] propose using $u_p = -k_p \arctan(\theta)$ and $u_d = -k_d \arctan(\omega)$, where θ is the joint angle and $\omega = \dot{\theta}$ is the angular velocity of the joint. This ensures that $|\tau_c| \leq k_p + k_d$, thereby avoiding actuator saturation. For the attitude control of spacecraft, the authors of [13] propose using proportional and derivative control similar to $u_p = -k_p \frac{p}{\sqrt{1+p^2}}$ and $u_d = -k_d \tanh(\omega)$, where $p = \tan(\theta/2)$ is a Gibbs parameter. This paper proposes adapting the work of [13] to be used to control a single-link flexible-joint robotic manipulator, as well as introducing alternative control laws.

To motivate the structure the proposed controller, recall that the Gibbs parameter, $\mathbf{p} \in \mathbb{R}^3$, is related to Euler axis/angle variables by

$$\mathbf{p} = \mathbf{a} \tan(\theta/2). \tag{2}$$

The relationship between the angular velocity and the time rate of change of the Gibbs parameter is [16]

$$\dot{\mathbf{p}} = \tfrac{1}{2}\left(\mathbf{1} + \mathbf{p}^{\times} + \mathbf{p}^{\mathsf{T}}\mathbf{p}\right)\boldsymbol{\omega}. \tag{3}$$

Considering only rotation about a single axis, Eqs. (2) and (3) simplify to

$$p = \tan(\theta/2), \tag{4}$$

$$\dot{p} = \tfrac{1}{2}\left(1 + p^2\right)\omega. \tag{5}$$

These properties will assist in the selection of alternative control laws and in proving stability.

The one-link flexible-joint robotic manipulator presented in Section 2 rotates about a single axis, which allows the work of [13] to be adapted in the following way. First, u_p and u_d are specified as

$$u_p = -k_p f(p), \tag{6}$$

$$u_d = -k_d \tanh(\omega), \tag{7}$$

where $f(x) = \frac{x}{\sqrt{1+x^2}}$, p is a Gibbs parametrization of the joint angle θ. Note that both $f(p)$ and $\tanh(\omega)$ are bounded by -1 and 1, which constrains the torque of the actuator to be less than the sum of k_p and k_d, that is $|\tau_c| \leq k_p + k_d$. This property ensures actuator saturation is avoided, as long as k_p and k_d are chosen to add up to less than the maximum torque that the actuator can apply.

An alternative control formulation is

$$u_p = -k_p f(\theta/2), \tag{8}$$

$$u_d = -k_d f(\omega). \tag{9}$$

Eqs. (8) and (9) are slight variations of Eqs. (6) and (7), where p is replaced by $\theta/2$ and $\tanh(\omega)$ is replaced by $f(\omega)$.

The four proposed control laws to be investigated are

$$-\tau_c = k_p f(p) + k_d f(\omega), \tag{10}$$

$$-\tau_c = k_p f(p) + k_d \tanh(\omega), \tag{11}$$

$$-\tau_c = k_p f(\theta/2) + k_d f(\omega), \tag{12}$$

$$-\tau_c = k_p f(\theta/2) + k_d \tanh(\omega). \tag{13}$$

Note that $\theta/2$ is used to match the linearization of $p = \tan(\theta/2)$ about $\theta = 0$ deg. A comparison of the relative control effort supplied by each option is presented in Fig. 2. The function $\frac{2}{\pi}\arctan(\pi\theta/4)$ is included in Fig. 2 to serve as a comparison to a controller found in literature [11]. The factors $\frac{2}{\pi}$ and $\pi/4$ were added to the arctan function in order to also match the linearization of $p = \tan(\theta/2)$ about $\theta = 0$ deg.

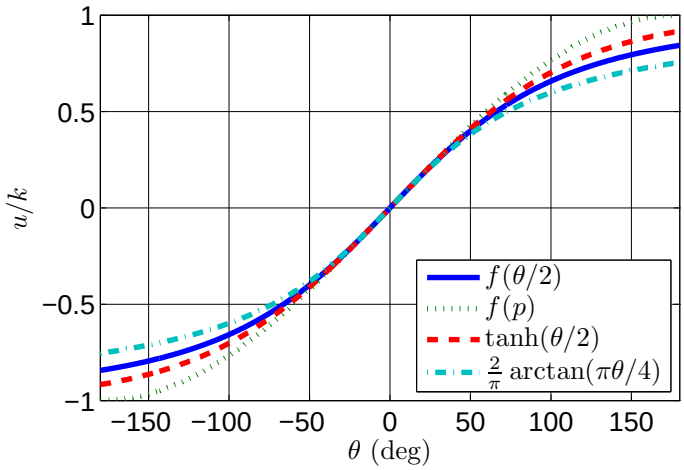

Fig. 2. Relative control effort versus θ.

Fig. 2 serves as motivation to use $f(p)$ for proportional control, due to its nonlinearity and relative aggressiveness further away from $\theta = 0$ deg. This larger relative control effort should allow the controller to drive the system to the desired equilibrium quicker.

3.2. Stability Analysis

We will now consider the closed-loop stability properties of the manipulator given in Eq. (1), and the four control laws given in Eqs. (10) to (13), each of which disallow the possibility of actuator saturation when the gains k_p and k_d are chosen appropriately. The control laws given by Eqs. (10) and (11) will be considered first.

Theorem 1. The dynamics of the single-link flexible-joint robot found in Eq. (1) on the domain $-\pi < \theta < \pi$, $-\pi < \alpha < \pi$, $\dot{\theta} \in \mathbb{R}$, $\dot{\alpha} \in \mathbb{R}$ together with the control laws given by Eqs. (10) and (11) render the equilibrium point $(\mathbf{q}, \dot{\mathbf{q}}) = (\mathbf{0}, \mathbf{0})$ of the closed-loop system asymptotically stable.

Proof. First, note that it can be easily shown using Eq. (1) and either Eq. (10) or Eq. (11) that $(\mathbf{q}, \dot{\mathbf{q}}) = (\mathbf{0}, \mathbf{0})$ is in fact an equilibrium point of the closed-loop system. Next, consider the Lyapunov function candidate:

$$V = \tfrac{1}{2}\dot{\mathbf{q}}^{\mathsf{T}}\mathbf{M}\dot{\mathbf{q}} + \tfrac{1}{2}\mathbf{q}^{\mathsf{T}}\mathbf{K}\mathbf{q} + 2k_p\left(1 - \frac{1}{\sqrt{1+p^2}}\right).$$

Taking the derivative of V and simplifying using Eqs. (1) and (5) yields

$$\begin{aligned}
\dot{V} &= \tfrac{1}{2}\left(\ddot{\mathbf{q}}^{\mathsf{T}}\mathbf{M}\dot{\mathbf{q}} + \dot{\mathbf{q}}^{\mathsf{T}}\mathbf{M}\ddot{\mathbf{q}}\right) + \tfrac{1}{2}\left(\dot{\mathbf{q}}^{\mathsf{T}}\mathbf{K}\mathbf{q} + \mathbf{q}^{\mathsf{T}}\mathbf{K}\dot{\mathbf{q}}\right) + 2k_p\frac{p\dot{p}}{(1+p^2)^{3/2}} \\
&= \dot{\mathbf{q}}^{\mathsf{T}}\mathbf{M}\ddot{\mathbf{q}} + \dot{\mathbf{q}}^{\mathsf{T}}\mathbf{K}\mathbf{q} + 2k_p\frac{p\left(\frac{1}{2}(1+p^2)\omega\right)}{(1+p^2)^{3/2}} \\
&= \dot{\mathbf{q}}^{\mathsf{T}}\left(\mathbf{M}\ddot{\mathbf{q}} + \mathbf{K}\mathbf{q}\right) + k_p\frac{p\omega}{\sqrt{1+p^2}} \\
&= \dot{\mathbf{q}}^{\mathsf{T}}\hat{\mathbf{b}}\boldsymbol{\tau}_c - \dot{\mathbf{q}}^{\mathsf{T}}\mathbf{D}\dot{\mathbf{q}} + k_p\frac{p\omega}{\sqrt{1+p^2}} \\
&= -\dot{\mathbf{q}}^{\mathsf{T}}\mathbf{D}\dot{\mathbf{q}} + \omega\left(-k_p\frac{p}{\sqrt{1+p^2}} - k_d h(\omega)\right) + k_p\frac{p\omega}{\sqrt{1+p^2}} \\
&= -\dot{\mathbf{q}}^{\mathsf{T}}\mathbf{D}\dot{\mathbf{q}} - k_d h(\omega)\omega,
\end{aligned}$$

where $h(\omega)\omega = \frac{\omega^2}{\sqrt{1+\omega^2}}$ when using Eq. (10), and $h(\omega)\omega = \omega\tanh(\omega)$ when using Eq. (11). Owing to the fact that $\dot{V}$ is negative semidefinite, the closed-loop system is stable. To show that the closed-loop system is asymptotically stable we will employ LaSalle's Invariant Set Theorem [17]. Notice that $\dot{V} = 0$ only if $\dot{\mathbf{q}} = \mathbf{0}$ (because $\mathbf{D}$ is positive definite), which implies that $\mathbf{q} = \mathbf{0}$ and $\tau_c = 0$. From LaSalle's Invariant Set Theorem it follows that the equilibrium point $(\mathbf{q}, \dot{\mathbf{q}}) = (\mathbf{0}, \mathbf{0})$ is asymptotically stable [17]. □

Theorem 2. The dynamics of the single-link flexible-joint robot found in Eq. (1) on the domain $-\pi < \theta < \pi$, $-\pi < \alpha < \pi$, $\dot{\theta} \in \mathbb{R}$, $\dot{\alpha} \in \mathbb{R}$ together with the control laws given by Eqs. (12) and (13) render the equilibrium point $(\mathbf{q}, \dot{\mathbf{q}}) = (\mathbf{0}, \mathbf{0})$ of the closed-loop system asymptotically stable.

Proof. First, note that it can be easily shown using Eq. (1) and either Eq. (12) or Eq. (13) that $(\mathbf{q}, \dot{\mathbf{q}}) = (\mathbf{0}, \mathbf{0})$ is in fact an equilibrium point of the closed-loop system. Next, consider the Lyapunov function candidate:

$$V = \tfrac{1}{2}\dot{\mathbf{q}}^{\mathsf{T}}\mathbf{M}\dot{\mathbf{q}} + \tfrac{1}{2}\mathbf{q}^{\mathsf{T}}\mathbf{K}\mathbf{q} + k_p\left(\sqrt{1+(\theta/2)^2} - 1\right).$$

Taking the derivative of V and simplifying using Eqs. (1) and (5) yields

$$\begin{aligned}
\dot{V} &= \tfrac{1}{2}\left(\ddot{\mathbf{q}}^{\mathsf{T}}\mathbf{M}\dot{\mathbf{q}}+\dot{\mathbf{q}}^{\mathsf{T}}\mathbf{M}\ddot{\mathbf{q}}\right)+\tfrac{1}{2}\left(\dot{\mathbf{q}}^{\mathsf{T}}\mathbf{K}\mathbf{q}+\mathbf{q}^{\mathsf{T}}\mathbf{K}\dot{\mathbf{q}}\right)+k_p\frac{\theta/2}{\sqrt{1+(\theta/2)^2}}\dot{\theta} \\
&= \dot{\mathbf{q}}^{\mathsf{T}}\left(\mathbf{M}\ddot{\mathbf{q}}+\mathbf{K}\mathbf{q}\right)+k_p\frac{\theta/2}{\sqrt{1+(\theta/2)^2}}\omega \\
&= \dot{\mathbf{q}}^{\mathsf{T}}\hat{\mathbf{b}}\boldsymbol{\tau}_c-\dot{\mathbf{q}}^{\mathsf{T}}\mathbf{D}\dot{\mathbf{q}}+k_p\frac{\theta/2}{\sqrt{1+(\theta/2)^2}}\omega \\
&= -\dot{\mathbf{q}}^{\mathsf{T}}\mathbf{D}\dot{\mathbf{q}}+\omega\left(-k_p\frac{\theta/2}{\sqrt{1+(\theta/2)^2}}-k_d h(\omega)\right)+k_p\frac{\theta/2}{\sqrt{1+(\theta/2)^2}}\omega \\
&= -\dot{\mathbf{q}}^{\mathsf{T}}\mathbf{D}\dot{\mathbf{q}}-k_d h(\omega)\omega,
\end{aligned}$$

where $h(\omega)\omega=\frac{\omega^2}{\sqrt{1+\omega^2}}$ when using Eq. (12), and $h(\omega)\omega=\omega\tanh(\omega)$ when using Eq. (13). Owing to the fact that $\dot{V}$ is negative semidefinite, the closed-loop system is stable. To show that the closed-loop system is asymptotically stable we will employ LaSalle's Invariant Set Theorem [17]. Notice that $\dot{V}=0$ only if $\dot{\mathbf{q}}=\mathbf{0}$ (because $\mathbf{D}$ is positive definite), which implies that $\mathbf{q}=\mathbf{0}$ and $\tau_c=0$. From LaSalle's Invariant Set Theorem it follows that the equilibrium point $(\mathbf{q},\dot{\mathbf{q}})=(\mathbf{0},\mathbf{0})$ is asymptotically stable [17]. □

Note that this stability analysis holds for any numerical system parameters, provided that $\mathbf{D}=\mathbf{D}^{\mathsf{T}}>0$ is positive definite, ensuring the controllers are robust to modelling errors. Assuming that $\mathbf{D}=\mathbf{D}^{\mathsf{T}}>0$ is positive definite is reasonable since there will always be some residual friction in the flexible-link system.

4. EXPERIMENTAL RESULTS

The proposed controllers are now validated experimentally by testing them on a rotary flexible-joint experimental testbed built by Quanser Consulting Inc [18]. The testbed has numerical values of $J_1=2.08\times10^{-3}$ (kg·m^2), $J_2=3.28\times10^{-3}$ (kg·m^2), $k_s=1.3$ (N·m/rad), $d_1=4\times10^{-3}$ (N·m/(rad/s)), and $d_2=1\times10^{-6}$ (N·m/(rad/s)). The base of the flexible joint is fixed, while the hub and link are rotated by an angle θ and α respectively. All control laws were tested on the nominal system and the perturbed system, as shown in Fig. 3. The perturbed system has a link inertia that is approximately 22 % greater than that of the nominal system.

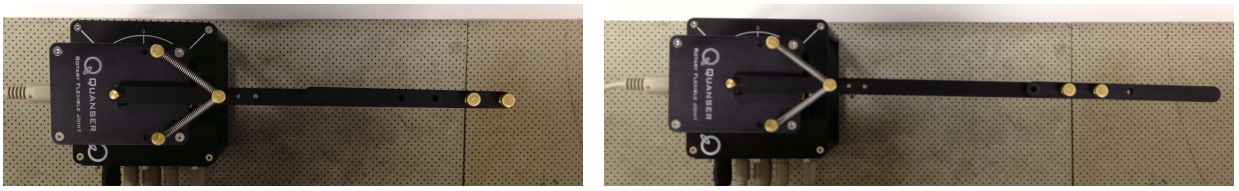

(a) (b)

Fig. 3. (a) Nominal and (b) perturbed experimental systems.

4.1. Set-Point Regulation

A step input of 90 degrees was given as a set point to the controller. In these tests $k_p=0.6$ (N·m) and $k_d=0.15$ (N·m), which guarantees $|\tau_c|\leq 0.75$ (N·m). In Fig. 4 is the θ versus time responses for the four proposed controllers. In Fig. 5 are the θ and α responses, u_p, the applied proportional torque, and u_d, the

applied derivative torque versus time for all proposed controllers and a controller found in [11]. Note that the functions $g(\theta/2)$ and $g(\omega)$ in the legend of Fig. 5 represent $\arctan(\pi\theta/4)$ and $\arctan(\pi\omega/2)$ respectively. In Fig. 6 are the θ and α responses, u_p versus time, and u_d versus time of the perturbed system.

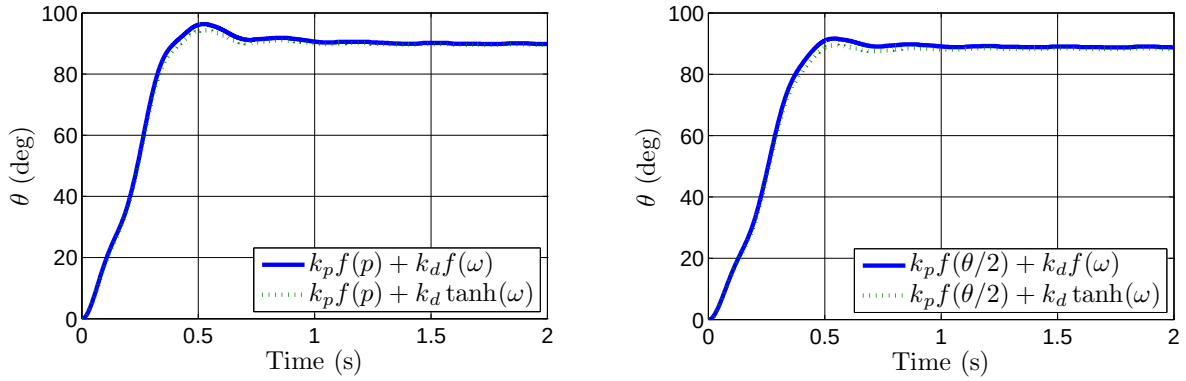

(a) (b)

Fig. 4. θ versus time.

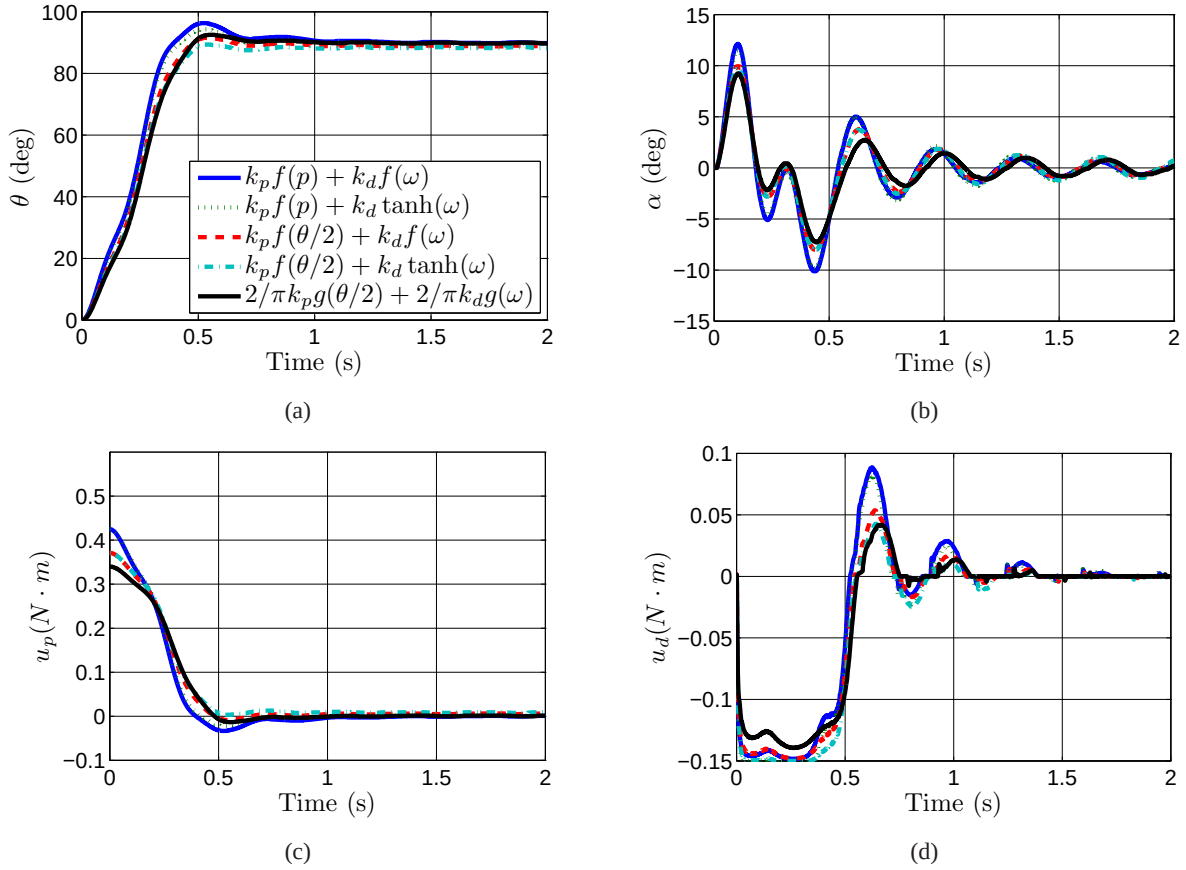

(a) (b)

(c) (d)

Fig. 5. Nominal system experimental set-point regulation results: (a) θ versus time, (b) α versus time, (c) u_p versus time, and (d) u_d versus time.

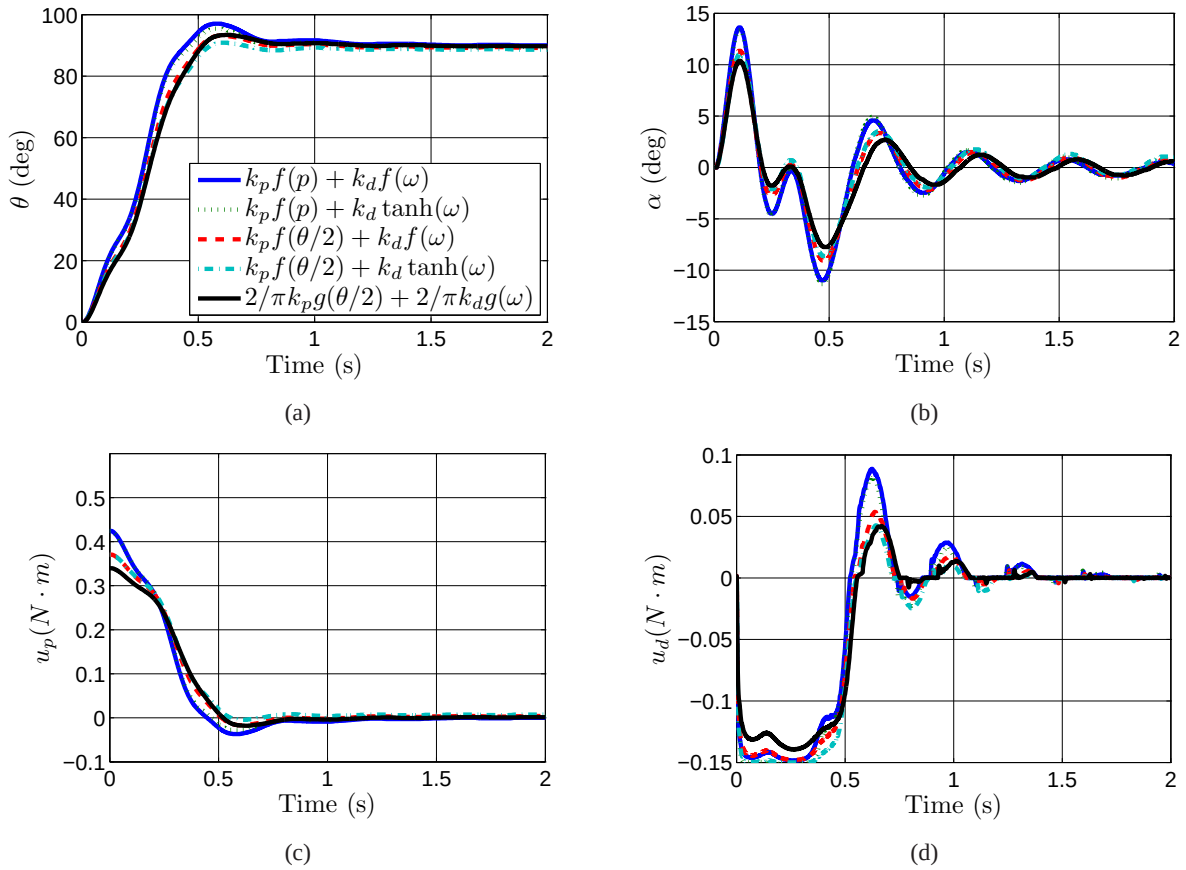

Fig. 6. Perturbed system experimental set-point regulation results: (a) θ versus time, (b) α versus time, (c) u_p versus time, (d) u_d versus time.

4.2. Trajectory Tracking

Trajectory tracking will now be considered. Consider the following desired trajectory, which can be found by interpolating a fifth order polynomial to satisfy a set of boundary conditions:

$$\theta_d(t) = \left[10\left(\frac{t}{t_f}\right)^3 - 15\left(\frac{t}{t_f}\right)^4 + 6\left(\frac{t}{t_f}\right)^5\right](\theta_f - \theta_i) + \theta_i, \tag{14}$$

where θ_i is the initial position of θ, θ_f is the final position of θ, and t_f is the time required to move from θ_i to θ_f. This desired trajectory in Eq. (14) was input to the various controllers tested as a reference input. Values of $\theta_i = 0$ deg, $\theta_f = 90$ deg and $t_f = 1$ second were used during the experiments. The controllers were tuned to $k_p = 1.7$ (N·m) and $k_d = 0.05$ (N·m), which guarantees $|\tau_c| \leq 1.75$ (N·m). Note that although experimental trajectory tracking results are presented, the asymptotic stability of our controllers subject to a tracking input has not been proven. In Fig. 7 is the θ and α response of the system, as well as u_p and u_d versus time. Figure 8 shows the same information for the perturbed system. Note that Figs. 7 and 8 use the same legend presented in Figs. 5 and 6 with the addition of the desired trajectories in Figs. 7(a) and 8(a).

4.3. Discussion

The results of the experimental tests show that the proposed controllers behave quite similarly to an existing controller taken from [11], which was also used for saturation avoidance. As expected, the controllers

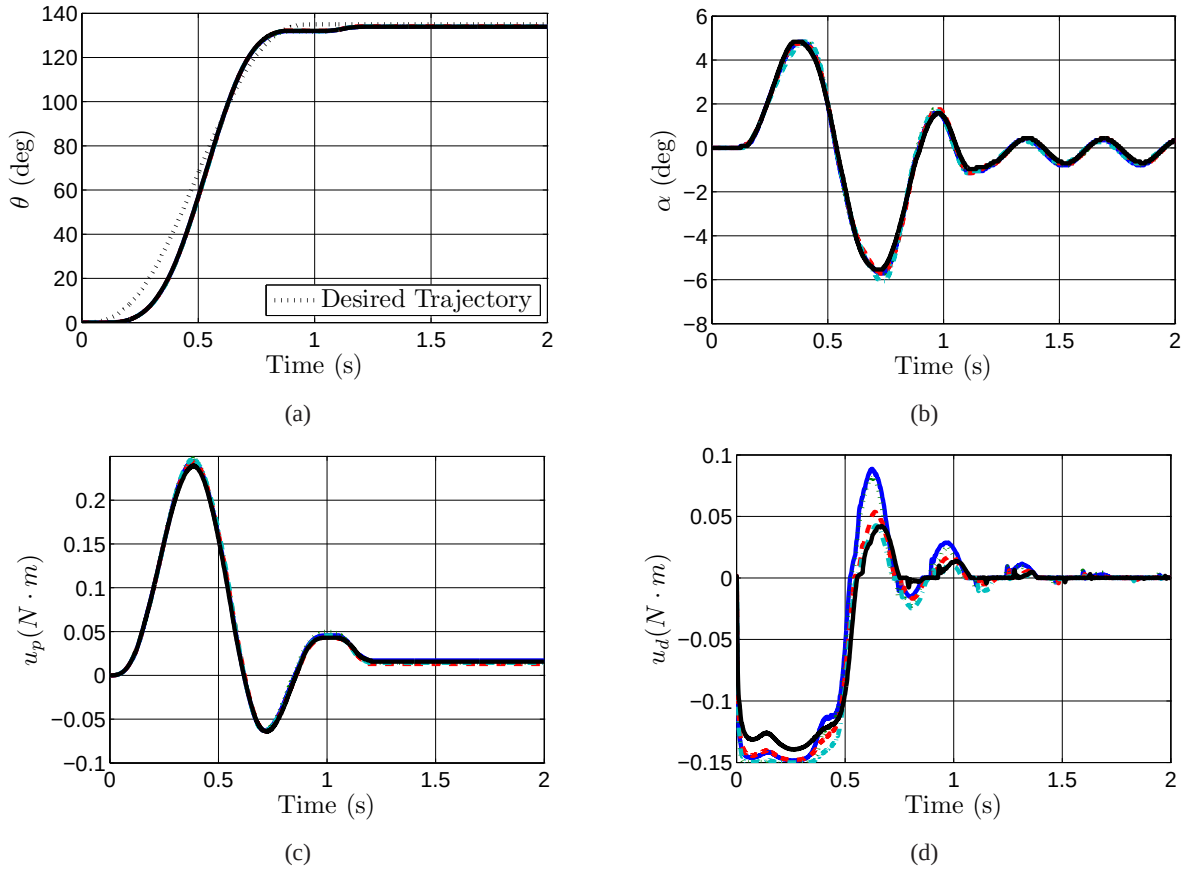

Fig. 7. Nominal system experimental tracking results: (a) θ versus time, (b) α versus time, (c) u_p versus time, (d) u_d versus time.

that are shown to be more aggressive in Fig. 2 do result in more overshoot in the set-point experiment, while having a slightly shorter settling time. In the tracking experiments the controllers gave almost identical system responses. The joint angle was never more than 20 degrees away from the trajectory it was tracking, which meant all controllers were within the linear region between -20 deg $< \theta < +20$ deg seen in Fig. 2 where all controllers are identical, which explains the almost identical results. Figures 5(d), 6(d), 7(d) and 8(d) show that not all controllers allow the actuator to fully saturate. It is interesting to note that although the controllers provide relatively different derivative control, the system responses are quite similar. The use of the function $f(x)$ in the control architecture is attractive, since it is computationally easier to compute than $\tanh(x)$ or $\arctan(x)$, while maintaining a similar system response.

5. CONCLUSIONS

This paper has investigated the control of a single-link flexible-joint robotic manipulator using various controllers that assure actuator saturation avoidance. Moreover, it was shown that the proposed controllers render the desired equilibrium point of our closed-loop system asymptotically stable. The experimental results suggest that the proposed controllers perform similarly to saturation avoidance controllers found in literature, but this may not necessarily be true in all conditions. It is also worth mentioning that $f(x)$ is computationally easier to compute than $\tanh(x)$ or $\arctan(x)$, which is crucial in robotic applications with limited computational hardware.

Although this paper dealt with a one-link flexible-joint robotic manipulator, this should be extended in future work to include multi-link robotic manipulators. Such an extension would allow the proposed controllers to be implemented on a wide range of robotic manipulators.

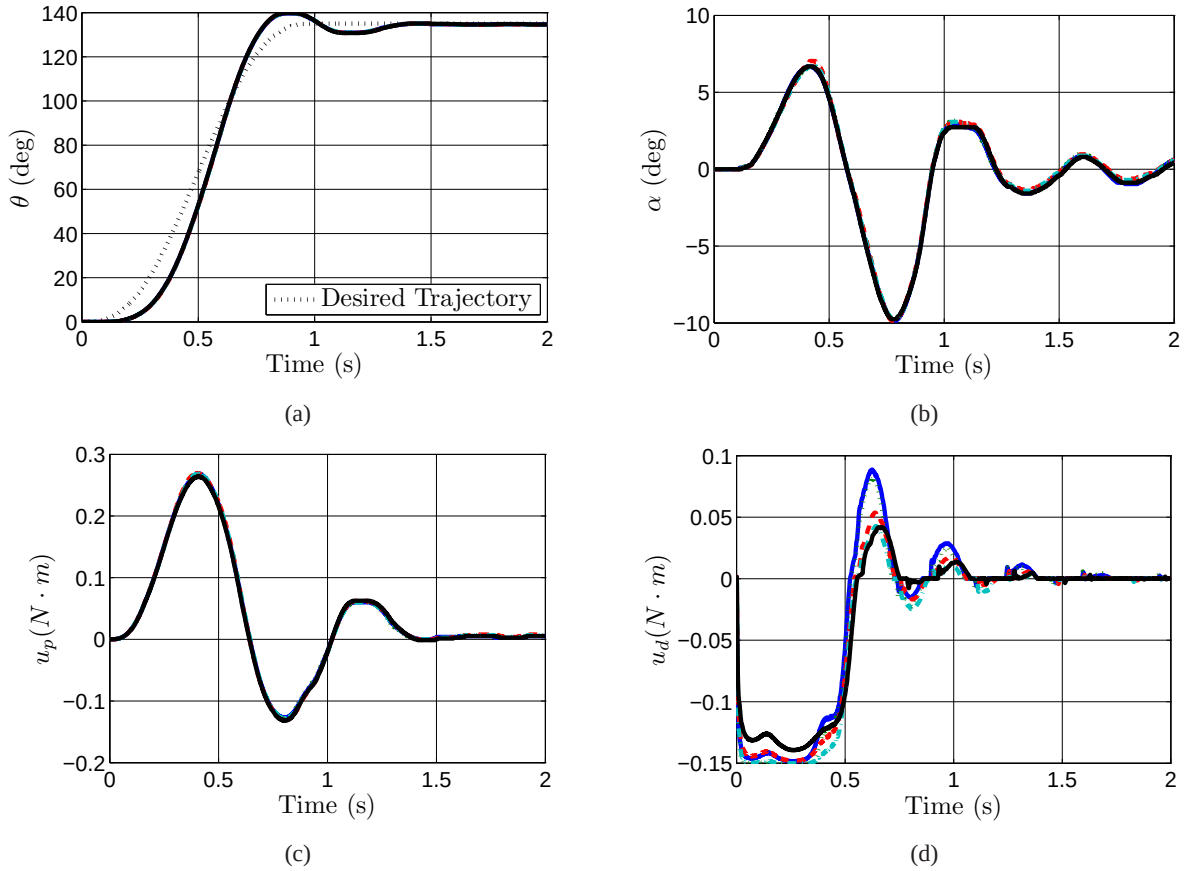

Fig. 8. Perturbed system experimental tracking results: (a) θ versus time, (b) α versus time, (c) u_p versus time, (d) u_d versus time.

REFERENCES

1. Rivin, E.I. *Mechanical Design of Robots*. Mcgraw-Hill, 1987.
2. Kelly, R., Santibáñez, V. and Loría, A. *Control of Robot Manipulators in Joint Space*. Springer, 2005.
3. Eppinger, S.D. and Seering, W.P. "Three dynamic problems in robot force control." *IEEE Transactions on Robotics and Automation*, Vol. 8, No. 6, pp. 751–758, 1992.
4. Ortega, R., Kelly, R. and Loría, A. "A class of output feedback globally stabilizing controllers for flexible joints robots." *IEEE Transactions on Robotics and Automation*, Vol. 11, No. 5, pp. 766–770, 1995.
5. Tomei, P. "A simple PD controller for robots with elastic joints." *IEEE Transactions on Automatic Control*, Vol. 36, No. 20, pp. 1208–1213, 1991.
6. Ulrich, S. and Sasiadek, J.Z. "Modeling and direct adaptive control of a flexible-joint manipulator." *Journal of Guidance, Control, and Dynamics*, Vol. 35, No. 1, pp. 25–39, 2012.
7. Ailon, A. and Ortega, R. "An observer-based set-point controller for robot manipulators with flexible joints." *Systems and Control Letters*, Vol. 21, pp. 329–335, 1993.
8. Aldu-Schäffer, A., Ott, C. and Hirzinger, G. "A unified passivity-based framework for position, torque and impedance control of flexible join robots." *The International journal of Robotics Research*, Vol. 26, No. 1, pp. 23–39, 2007.

9. Maeda, K., Tadokoro, S., Takamori, T., Hiller, M. and Verhoeven, R. "On design of a redundant wire-driven parallel robot warp manipulator." In "Proceedings of the IEEE International Conference on Robotics and Automation," pp. 895–900. Detroit, Michigan, USA, May 10–15 1999.
10. Ortega, R., Loría, A., Nicklasson, P.J. and Sira-Ramirez, H.J. *Passivity-based control of Euler-Lagrange systems*. Springer, 1998.
11. Liu, H., Zhu, S. and Chen, Z. "Saturated output feedback tracking control for robot manipulators via fuzzy self-tuning." *Journal of Zhejiang University-SCIENCE C (Computers and Electronics)*, Vol. 11, No. 12, pp. 956–966, 2010.
12. Moreno-Valenzuela, J. and Santibáñez, V. "Robust saturated PI joint velocity control for robot manipulators." *Asian Journal of Control*, Vol. 15, No. 1, pp. 64–79, 2013.
13. Su, Y. and Zheng, C. "Globally asymptotic stabilization of spacecraft with simple saturated proportional-derivative control." *Journal of Guidance, Control, and Dynamics*, Vol. 34, No. 6, pp. 1932–1935, 2011.
14. Tsiotras, P. and Luo, J. "Control of underactuated spacecraft with bounded inputs." *Automatica*, Vol. 36, No. 8, pp. 1153–1169, 2000.
15. Boskovic, J.D., Li, S.M. and Mehra, R.K. "Robust adaptive variable structure control of spacecraft under control input saturation." *Journal of Guidance, Control, and Dynamics*, Vol. 24, No. 1, pp. 14–22, 2001.
16. Hughes, P.C. *Spacecraft Attitude Dynamics*. 2 ed.. Dover, 2004.
17. Slotine, J.J.E. and Li, W. *Applied Nonlinear Control*. Prentice-Hall, 1991.
18. Quanser Consulting Inc. Quanser Rotary Servo User Manual, 2011.